Bond Strength of Tension Lap-Splices in Full Scale Self-Compacting Concrete Beams

Kâzım TÜRK
Harran University, Civil Engineering Department, Şanlıurfa-TURKEY
e-mail: kturk@harran.edu.tr
Ahmet BENLİ
Bingöl University, Bingöl Vocational High School, Bingöl-TURKEY
Yusuf CALAYIR
Fırat University, Civil Engineering Department, Elazığ-TURKEY

Abstract

Twelve full-scale beam specimens (2000 × 300 × 200 mm) were tested in positive bending with the loading system designed to determine the effect of self-compacting concrete (SCC) and the diameter of reinforcement on bond-slip characteristics of tension lap-slices. The specimens of lap-splice series were tested with lap-spliced bars centred on the midspan in a region of constant positive bending. The splice length of the deformed bars was set at 310 mm in all beam specimens. This value was selected to develop a steel stress less than yield to ensure splitting mode failure in all beam specimens. The beams were cast with the 16 and 20 mm bars (the tension lap-splices) in the bottom position. The casting procedure was the same for all beams. Two types of concrete were used in the experimental programme, including normal concrete (NC), with a slump less than 68 mm, as the comparatively low-slump concrete, and SCC as an extremely high-workability concrete. The variables used in this study were the concrete type (SCC and NC) and reinforcing bar size (16 and 20 mm). It was found that as the diameter of the steel bar increased from 16 to 20 mm the bond strength decreased regardless of concrete type. Finally, although the compressive strength of concretes was almost the same and there were slight differences between the diameters of lap-spliced bars, the normalised bond strengths of the SCC mixes were about 4% higher than those of the NC mixes for both bar diameters, indicating that the reinforcing bar was completely covered by SCC due to its filling ability.

Key Words: Self-compacting concrete, Bond strength, Lap splice, Full-scale beam, Positive bending.

Introduction

When a reinforced concrete (RC) member is subjected to loading, the load is transferred between the main reinforcement and the surrounding concrete through adhesional and mechanical bonds. If deformed bars are used, a mechanical bond is provided by the bar lugs bearing against the surrounding concrete. The consolidation of the surrounding concrete in congested RC members is an important consideration in concrete placement and durability of structures. Achieving proper consolidation can require internal and external vibration. With the in-creasing use of congested reinforcement in moment-resisting members, for example, due to seismic consideration, there is a growing interest in specifying high workability concrete. Self-compacting concrete (SCC) in the fresh state is known for its excellent deformability, high resistance to segregation, and use, without applying vibration, in congested reinforced concrete structures characterised by difficult casting conditions. SCC is defined as concrete that can be placed normally by pump or skip, and flow under its own weight, maintaining its homogeneity. It will completely fill the formwork of shape, even with congested reinforcement, subjected to the ag-

gregate size. Full compaction and in-situ strength are achieved without the assistance of mechanical vibration (Okamura and Ozawa, 1995). In general, the mixture proportion of SCC includes mineral additives, such as silica fume, fly ash and slag, as well as chemical admixtures, such as high-range water reducing (HRWR) admixtures and/or viscosity modifying agents (VMA), to adjust its deformability and cohesiveness. The use of SCC can remarkably lower the complexity of construction by reducing the demand for a significant amount of consolidation practice and skilful workmanship. Therefore, the self-consolidation characteristics of SCC allow a much easier construction schedule and result in a more reliable quality in concrete placement and a more homogeneous material structure. Without consolidation, the influence of intrinsic deficiencies and material defects due to bleeding or segregation induced by improper vibration practice can be avoided (Hoshino, 1989). As a result, the homogeneity of SCC can be ensured and may substantially enhance the mechanical properties of RC members. In other words, the uncertainties in RC structures caused by construction factors can be effectively eliminated. Therefore, the designed structural performance and the expected durability can be enhanced.

In a study dealing with pull-out tests, Chan et al. (2003) reported that, as compared to NC, SCC exhibits higher bond to reinforcing bars and lower reduction in bond strength due to the top-bar effect. Zhu et al. (2004) performed bond tests (pull-out tests) with 12 and 20 mm deformed bars placed in concrete specimens of $100 \times 100 \times 150$ mm to study the performance of SCC compared to NC. The test results showed 10%-40% higher normalised bond strength in SCC compared to NC. Several factors affecting the bond strength have been studied by a number of researchers. These factors include the loading condition, the size reinforcement, the composition materials, compressive strength of concrete (Ezeldin and Balaguru, 1989; Azizinamini et al., 1993; Yerlici and Özturan, 2000; Turk and Yildirim, 2003; Turk et al., 2005; Esfahani et al., 2008) and testing methods and apparatus (Darwin et al., 1996; Hwang et al., 1996; Esfahani and Rangan, 1998), whilst there are very limited data on the bond strength of tension lap-splices in SCC.

This paper reports an investigation aimed at evaluating the bond strength of tension lap-spliced bars in full-scale beams produced from SCC and comparing them in conventional vibrated concrete.

Experimental Programme

Materials

The concrete mixes used in this study were prepared with 42.5N grade Portland Cement (PC), and silica fume (SF) from set cement factory in Elazığ, and Electro Metallurgy Enterprise in Antalya, Turkey, respectively. Aggregate was obtained from the River Murat in Elazığ, Turkey. The silica fume was of high fineness (96.5% < 45 μm). The silica fume was used as additional filler in SCC to enhance self-compactability and segregation resistance.

Natural sand and gravel with a nominal maximum size of 20 mm were used as the aggregates. Medium grade natural sand with a fineness modulus of 3.05 was also used for both mixes. The relative density values for 0-7, 7-15, and 15-20 were 2.63, 2.64, and 2.66, and absorption rates were 1.57%, 1.0%, and 0.7%, respectively. Melamine sulfonate polymer based and modified polycarboxylates based polymer were used, which had specific gravity of 1.22 and 1.06, for NC and SCC, respectively.

Proportions of mixes used

Two types of concrete were used in the experimental programme, including NC and SCC. Details of mix proportions for the conventional and the SCC are summarized in Table 1. A typical mixture proportion of NC is selected with moderate water-cement ratio (w/c) and workability. While the NC mix contains only ordinary PC, the SCC mix contains 10% silica fume by weight of cement to enhance fluidity and cohesiveness, as well as a particular type high range-water-reducing admixture adopted to achieve self-compactability.

The fresh concrete properties of the 2 different concretes are summarised in Table 2. The slump of NC is 68 mm as measured before casting. In addition to the slump, there are several other essential test items for fresh concrete properties of SCC based on guidance given in EFNARC (2005), including the slump flow, T_{50}, V-funnel test, L-box test, and segregation sieve test. A slump flow of 701 mm is measured for SCC, indicating good deformability. The discharge time from the V-funnel provides an index of viscosity of SCC. Finally, while the L-box test verifies the self-compactability, the segregation sieve test demonstrates segregation resistance of SCC. The results obtained from these tests (Table 2) show that

the SCC mix has good flow, filling, and passing ability as well as segregation resistance.

Experimental procedures

Twelve geometrically identical beam specimens were tested in positive bending with the loading system designed to produce a constant moment region in the middle of the beam specimen. The geometrical details and compressive strength values of concretes at 28 days are given in Table 3.

Reinforcement on the tension side consisted 2 reinforcing bars spliced at the centre of the span. The beams, which had 2 lap spliced bars of 16 or 20 mm in tension, were cast in the bottom position. The thickness of the cover concrete was measured from the centre of the stirrup to the nearest surface of the concrete (Figure 1).

The casting procedure was the same for all beams. The splice length of the deformed bars was set at 310 mm in all beam specimens. This value was selected to develop a steel stress less than yield to ensure splitting mode failure in all beam specimens. A yielding mode of failure provides little or

no information regarding the bond strength of a reinforcing bar, and the objective was to compare relative bond behaviour of lap splices and not ductility of the splices. The variables used in this study were the concrete type (NC and SCC) and reinforcing bar size (16 and 20 mm). A 3-part notation system was used to indicate the variables of each beam. The first part of the notation indicates the beam specimen. The second part is the concrete type (NC or SCC). The third is the diameter of reinforcement (16 and 20 mm). As an example of the notation system, B.SCC.20 indicates that the beam specimen was produced from SCC and had 20 mm bars (the tension lap splices). Two different diameters (16 and 20 mm) of steel reinforcement were selected, the mechanical properties of which are shown in Table 4. The bars used were from the same heat of steel and had the same parallel deformation pattern. The bars met TS 708 specifications and were Grade 60. The transverse reinforcement was provided in all beams to avoid shear failure. It consisted of 10 mm bars spaced at 8 cm centre-to-centre and the 2 top reinforcing bars extending along the entire beam length were 12 mm deformed bars (Figure 1).

Table 1. Mix proportions of concretes used during the experiments.

Mix	Materials, (kg/m^3) Cementitious	SF (%)	w/c	Aggregates, (kg/m^3)			SP (l /m^3)	SP (l /m^3)
				0-7	7-15	15-20		
NC	350	0	0.39	800	500	650	-	5.50
SCC	450	10	0.38^a	990	450	285	8.00	-

^{a}: water to cementitious materials (PC + SF) ratio

Table 2. Properties of fresh concretes.

Mix	Slump (mm)	T$_{50cm}$ (s)	V-funnel Flow time (s)	L-box H$_2$/ H$_1$	Segregation (%)
NC	68	-	-	-	-
SCC	701^b	1.80	3.19	0.876	17.9

^{b} Slump Flow (mm)

Table 3. Test parameters and details of beam specimens.

Mix Code	f'_c (MPa)	d_b (mm)	l_s (mm)	Number of Beams Tested	b (mm)	h (mm)	ρ [A$_b$/(b × d)]
B. NC.16	41.48	16	310	3	200	300	0.0116
B.NC.20	41.48	20	310	3	200	300	0.0158
B.SCC.16	43.11	16	310	3	200	300	0.0116
B.SCC.20	44.05	20	310	3	200	300	0.0158
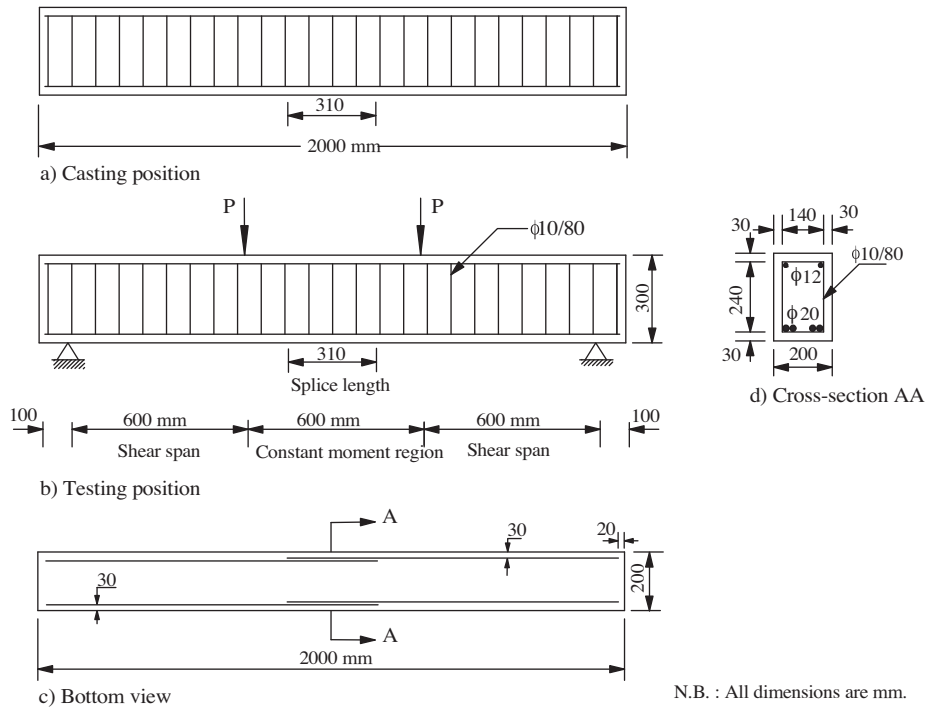
Figure 1. Views of the beam specimens in the casting and testing positions.

Table 4. Properties of steel reinforcement used.

d_b (mm)	A_b (mm^2)	f_y (MPa)	f_{su} (MPa)	Elongation percent
16	200.96	503.18	636.94	26.00
20	314.16	509.55	780.25	23.60

The SCC was poured into the mould at once without any vibration while the NC was cast in 2 layers in each beam specimen. As the beam specimen produced from NC was cast, a person was assigned to assess compaction and vibration to ensure that the concrete placed in each specimen was of the same consistency. A poker vibrator was used to attain optimum compaction. Test beams were cast in a horizontal position with the lap-spliced bars located at the bottom of the steel mould. Following casting, all beam specimens and the 150 mm concrete cubes were covered with wet burlap, which continued for 28 days following de-moulding the specimens after 24 h. All specimens were tested at 28 days.

The test set-up and the 4-point loading arrangement used during the load controlled experiments are given in Figure 2. Beams were simply supported over a span of 1800 mm and tested until failure took place. An incremental load of 3.5 kN/s was applied through a 250 kN capacity testing machine. The load from the testing machine was transferred through a stiff steel girder onto the specimens in the form of 2 equally concentrated loads.

At each load stage, deflection readings were taken at the centre of the beam using a dial gauge and flexural cracks were marked. Cracks at the side and bottom (tension) faces of the specimens were marked for further analysis. Concrete cover over the splice length in all specimens was first to fail due to the interfacial bond failure between reinforcement bars and concrete.

Test Results

Beam stiffness

Figure 3a and b, and c and d show typical plots of load vs. midspan deflection for each beam produced from NC and SCC, respectively. A dial gauge was placed at the centre of the beam span after placing the beam specimen. It was seen that whilst the diameter of the reinforcing bar was increased the maximum load increased and the deflection recorded at the centre of the beam decreased, regardless of the concrete type. As can be seen from Figure 3, the load vs. midspan deflection relationship was similar for each beam specimen, which indicates a good transfer of the load up to bond failure.
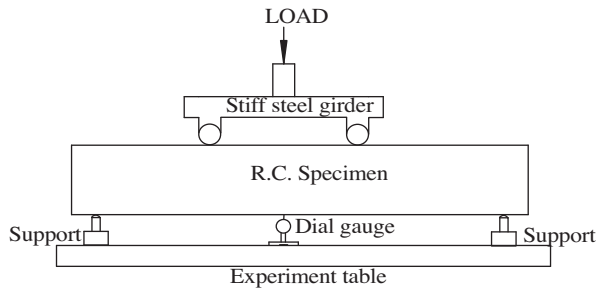
Figure 2. Schematic of test setup.

The average cracking load of the beams with SCC was approximately 65 kN, whilst that of the beams

with NC was around 56 kN for both reinforcement diameters. Furthermore, as loading increased above the cracking load, it can be seen from Figure 3 and Table 5 that the beam specimens produced from both NC and SCC with 20 mm tension lap-spliced bars had greater stiffness than did the beam specimens with 16 mm tension lap-spliced bars, because the beam specimens with 20 mm had greater load with 29.2 than did the beam specimens with 16 mm with 20.7 kN for 1 mm deflection. However, after the beams reached cracking load there were slight differences between the stiffnesses of all beam specimens for the same diameter bars.

a) B.NC.16

b) B.NC.20

c) B.SCC.16

d) B.SCC.20
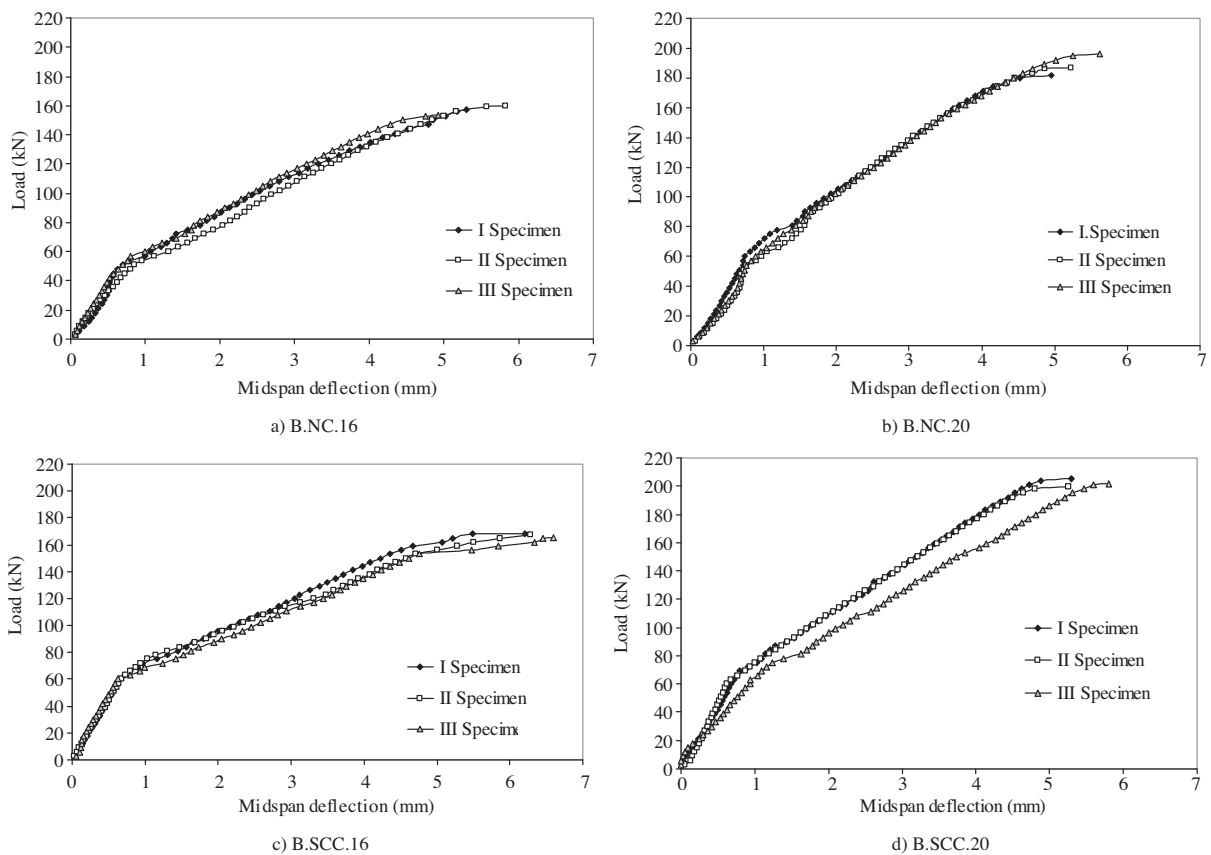
Figure 3. Load-deflection curves for beam specimens produced from NC and SCC.

Table 5. The values of load-midspan deflection of the beams during cracking and failure.

Specimens	During Cracking		During Failure	
	Load (kN)	Deflection (mm)	Load (kN)	Deflection (mm)
B. NC.16	54	0.81	156.9	5.35
B.NC.20	57	0.78	188.2	5.27
B.SCC.16	60	0.65	167	6.36
B.SCC.20	70.7	0.96	202	5.45

Cracking behaviour

In all specimens, failure diminishing of load carrying capacity took place at maximum load just after the longitudinal splitting cracks started to form along the splices. The final mode of failure was a face-and-side split failure. Failure developed gradually and was ductile especially compared to beams with NC and with no stirrups that were tested (Turk and Yildirim, 2003; Turk et al., 2005), because it can be seen from Figure 3 and Table 5 that the beam specimens with SCC had higher the midspan deflection than that of the beam specimens with NC for both 16 and 20 mm. This ductility occurs as a result of the transverse reinforcement and the SCC used in producing the beams, because SCC allowed most bar lugs to contribute to stress transfer between the bars and concrete in the splice region.

Cracking in the constant moment region consisted of vertical flexural cracks, while cracks outside the constant moment region developed as flexural vertical cracks at a lower load level but transformed into inclined shear cracks at higher load in all beams. The observed cracking patterns on the bottom tension face and on the side of all beam specimens were similar regardless of concrete type and reinforcement diameter. On the other hand, the longitudinal cracks formed at the bottom face and adjacent to the reinforcement bars and the cracks of the beams with SCC on the bottom tension face were more than those of the beams with NC (Figure 4a and b) since SCC covered the reinforcement sufficiently because of its filling ability.

a) B.NC.16
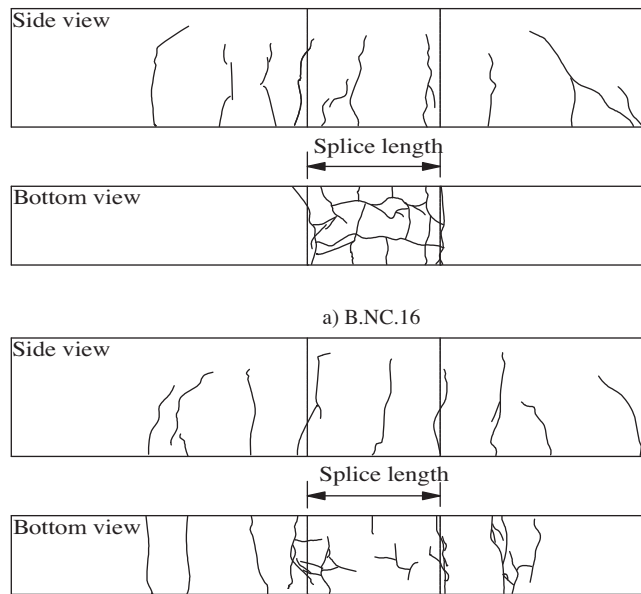
Figure 4. Crack patterns of the beams produced from NC and SCC.
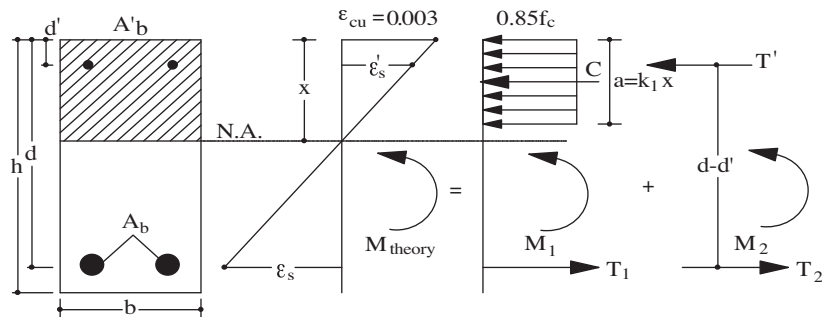
Figure 5. Strain and stress distribution in a RC beam cross-section.

Ultimate moment capacities

Table 6 shows the experimental and theoretical ultimate moment capacities of the reinforced concrete beams produced from NC and SCC. The theoretical ultimate moment was calculated using the limit state design equations, derived from stress and strain distributions as shown in Figure 5, and assuming the continuous presence of longitudinal bars (i.e. adequate splice length) as

$$M_{theor.} = A_b \times f_y \times \left(d - \frac{a}{2}\right) \qquad (1)$$

where $a = k_1 \times \chi$, and $k_1 = 0.85 - (f_{ck} - 25) \times 0.006$

The experimental moment was calculated as

$$M_{\exp} = P \times L \qquad (2)$$

It can be seen in Table 6 that the theoretically predicted ultimate moment capacity of the beams made of NC and SCC takes into account only approximately 80% and 84% of the rebar ultimate tensile strength, respectively, though all beam specimens had the same splice embedment length with 310 mm and there were no significant differences with approximately 2.1 MPa between the compressive strengths of the beams made of NC and SCC. This result is somewhat verified by Valcuende and Para (2009), who proposed a reduction in the anchorage length of reinforcements according to the concrete's compressive strength for SCC.

Bond strength

Using the limit state design equations (Dogangun, 2003), it is possible to calculate the tensile strength of the spliced rebar at failure, considering that the spliced rebar is acting as one continuous rebar. The failure mode in all beam specimens was a face-and-side split failure suggesting that the splice reached its maximum capacity. Therefore, bond strength could be determined directly from the stress developed in the steel. The stress in the steel, fs, was calculated based on elastic cracked section analysis and was determined from the maximum load obtained for each beam specimen. The analysis ignored the tensile stresses in the concrete below the neutral axis and assumed linear stress-strain behaviour. In this analysis the modulus of elasticity of steel, Es, was taken as 203,000 MPa and the modulus of elasticity of concrete was calculated as the average of 3 samples. The end faces of the samples are ground using an end-face grinder, and then checked for evenness and perpendicularity with respect to the vertical axis. To obtain the average bond stress, u_t, the total force developed in the steel bar ($A_b \times fs$, where A_b is the cross-sectional area of the bar) was divided by the surface area of the bar over the splice length ($\pi \mathrm{X} d_b \times ls$) as follows:

$$u_t = \frac{(A_b \times f_s)}{\pi \times d_b \times l_s} \; ; \; u_t = \frac{f_s \times d_b}{4 \times l_s} \qquad (3)$$

where d_b is the bar diameter and l_s is the splice length. Neutral axis width (c) and steel stress (f_s) are given in Table 6.

Table 6 also summarises the test results indicating the effect of the concrete type and the diameter of the reinforcing bar on bond strength. It can be clearly observed in Table 6 that as the diameter of the steel bar increased from 16 to 20 mm the bond strength decreased regardless of concrete type. However, a higher bond strength was obtained from the beams produced from SCC for both the diameters of 16 mm and 20 mm. Therefore, the normalised bond strengths of the SCC mixes were found to be about 4% and 3% higher than those of the NC mixes for the reinforcing bar of diameter 16 and 20 mm,

Table 6. Summary of test results.

Mix Code	f'_c (MPa)	$M_{\exp}$ (kN.m)	M_{theor} (kN.m)	δ (mm)	c (mm)	f_s (MPa)	$u_{\exp}$ (MPa)	$\dfrac{u_{\exp}}{\sqrt{f_c}}$	Mode of Failure
B. NC.16	41.48	47.07	52.10	5.35	32.97	463.71	5.98	0.93	Splitting
B.NC.20	41.48	56.47	81.94	5.27	37.46	358.23	5.78	0.90	Splitting
B.SCC.16	43.11	50.10	54.12	6.36	33.18	493.26	6.36	0.97	Splitting
B.SCC.20	44.05	60.60	81.92	5.45	38.43	384.22	6.20	0.93	Splitting

respectively, though the compressive strengths of NC and SCCs were almost the same and there were few differences between the diameters of lap-spliced bars used as variable. Hence, it can be concluded that the reinforcing bars were completely covered by SCC due to its filling ability when involving the reinforcement (Valcuende and Para, 2009).

For the test results, $(u/\sqrt{f_c})$ was plotted against $1/\phi$ in Figure 6.
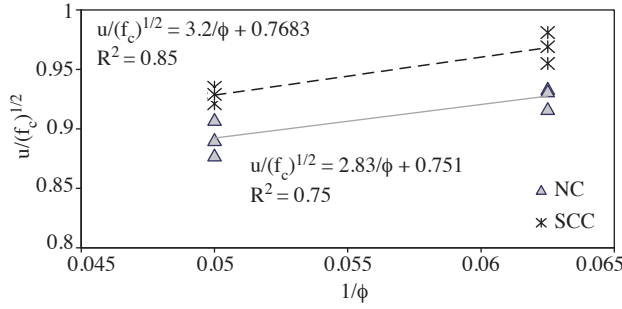
Figure 6. Proposed equations for bond strength for beam specimens with NC and SCC.

The best fit obtained from the test results is given for both NC and SCC. However, the fitted curve for SCC had the greater coefficient and the better correlation with $R^2 = 0.85$, indicating that there were less deviations between the bond values at beams with SCC due to its filling ability.

Comparison With Other Methods

Experimental bond strength results of the beams with 2 different diameters of reinforcement were compared to theoretically predicted values, by using the empirical equations developed by Orangun et al. (1977):

$$u = [1.2 + 3(c/d_b) + 50(d_b/l_s) + k'_{tr}]\sqrt{f_c} \quad (4)$$

where $k'_{tr} = \frac{A_{tr} \times f_{yt}}{500 \times s \times d_b}$, $\frac{c}{d_b} \leq 2.5$, $k'_{tr} \leq 3.0$

u theoretical bond stress, (psi)

c the smaller of c_b or c_s

c_b clear (bottom or side) cover to main reinforcement, (in.)

c_s half clear spacing between bars or splices or half available concrete width per bar or splice resisting splitting in the failure plane, (in.)

d_b diameter of reinforcing bar (in.)

f_c compressive strength of concrete, (psi)

k'_{tr} confinement factor, carries no units

A_{tr} area of transverse reinforcement crossing the potential plane of splitting adjacent of single anchored reinforcing bar, (in²)

f_{yt} specified yield strength of transverse reinforcement, (psi)

s centre-to-centre spacing of transverse reinforcement within splice length, (in.)

The constant 500 carries the unit (psi); 1 in. = 25.4 mm, and 1 MPa = 145 psi.

And by Esfahani and Rangan (1998):

$$U = u_c \frac{1 + 1/M}{1.85 + 0.024\sqrt{M}} \left(0.88 + 0.12\frac{c_{med}}{c_m}\right) \quad (5)$$

where $u_c = 4.9\frac{c_m/d_b + 0.5}{c_m/d_b + 3.6}f_{ct}$ for $f'_c < 50$ MPa, $u_c = 4.9\frac{c_m/d_b + 0.5}{c_m/d_b + 3.6}f_{ct}$ for $f'_c \geq 50$ MPa, and $M = \cosh\left(0.0022L_d\sqrt{R\frac{f'_c}{d_b}}\right)$, and U and f'_c are in Mpa; $f_{ct} = 0.55\sqrt{f'_c}$. c_m is the smallest value and c_{med} is the second larger value of side cover, bottom cover or $1/2$ of centre-to-centre spacing of bars. R varies between 3 and 4.25, depending on the type of reinforcing bar. U is equivalent uniform bond stress at failure (bond strength) and u_c is bond stress when the concrete cover cracks.

Moreover, experimental bond strength results of the beams were also compared to the equation developed by Darwin et al. (1996). The equation can be expressed in terms of u as

$$u = \frac{(f'_c)^{1/4}}{d_b \times \pi \times L_d}[63 \times l_s \times (c_m + 0.5 \times d_b) + 2130 \times A_b]\left(0.1\frac{c_M}{c_m} + 0.9\right) \quad (6)$$

in which $(f'_c)^{1/4}$ is psi.

c_m, c_M minimum and maximum value of c_s or c_b ($c_M/c_m \leq 3.5$), (in.)

c_s min ($c_{si} + 0.25$ in., c_{so}), (in.)

c_{si} one-half of clear spacing between bars, (in.)

c_{so}, c_b side cover and bottom cover of reinforcing bars, (in.)

A_b area of one reinforcing bar being spliced, (in².)

L_d development length (in.)

The results related to comparisons are given in Table 7. The measured bond stress for each specimen was divided by the predicted values to obtain the bond efficiencies listed in Table 7. The mean bond efficiency for all bar splices using Eq. (4) from Orangun et al. (1977) is 1.23 with a standard deviation of 0.002. Moreover, Eq. (5) from Esfahani and Rangan (1998) gives 1.35 with a standard deviation of 0.004, and Eq. (6) from Darwin et al. (1996)

Table 7. Bond efficiencies from Orangun et al. (1977), Esfahani and Rangan (1998), and Darwin et al. (1996).

Specimens	Measured bond stress, u_t (MPa)	Predicted bond stress (MPa)			Bond efficiency		
		Orangun et al.	Esfahani and Rangan	Darwin et al.	u_t/u_{Orangun}	u_t/u_{Esfahani}	u_t/u_{Darwin}
B. NC.16	5.98	4.99	4.60	4.77	1.20	1.30	1.25
B.NC.20	5.78	4.77	4.27	4.70	1.21	1.35	1.23
B.SCC.16	6.36	5.13	4.68	4.82	1.24	1.36	1.32
B.SCC.20	6.20	4.92	4.43	4.77	1.26	1.40	1.30

gives 1.28 with a standard deviation of 0.004. It is seen in Table 7 that whilst all the methods developed by other researches gave very good estimates of bond strength the predicted bond strength values using Eq. (4) were closer to the experimental values with the smallest standard deviation. However, it is clear that Eqs. (5) and (6) underestimate the bond strength between reinforcement and concrete in this study. On the other hand, the discrepancies between the measured bond stress and the values predicted by Eqs. (4), (5), and (6) may be attributed to the properties of materials, the geometric parameters of the specimen, the detailing of reinforcement, and the loading velocity during the experiments etc.

Conclusions

Based on the results of 12 beam specimens produced from NC and SCC with 2 lap-spliced bars 16 and 20 mm in diameter, the following conclusions can be drawn:

1. Whilst the diameter of the reinforcing bar was increased, the maximum load increased and the deflection recorded at the centre of the beam decreased, regardless of the concrete type. As loading increased above the cracking load, NC and SCC beam specimens with 20 mm tension lap-spliced bars had greater stiffness than the beam specimens with 16 mm, that is, the beam specimens with 20 mm had greater load with 29.2 kN than did the beam specimens with 16 mm with 20.7 kN for 1 mm deflection. However, there were slight differences between the stiffnesses of all beam specimens for the same diameter bars, after cracking load.

2. Load transfer within the tension lap-spliced bars embedded in SCC in a reinforced concrete beam was better than that of the tension lap-spliced bars embedded in NC. Moreover, failure developed gradually and was ductile especially in these beams compared to beam specimens produced from NC and with no stirrups, because it was concluded that SCC allowed most bar lugs to contribute to stress transfer between the bars and concrete in the splice region.

3. The beam specimens produced from SCC had generally longer cracks than the beams produced from NC regardless of the reinforcing bar diameter, indicating that SCC surrounded the reinforcing bar sufficiently due to its filling ability.

4. The normalised bond strengths of the SCC mixes were about 4% higher than those of the NC mixes for both bar diameters (16 and 20 mm), though there were few differences between the compressive strengths of normal and self-compacting concretes with approximately 2.1 MPa.

5. The experimental results were compared to those reported by Orangun et al. (1977), Esfahani and Rangan (1998), and Darwin et al. (1996). The method developed by Orangun et al. (1977) provides a better estimate of bond strength than those developed by Darwin et al. (1996) and Esfahani and Rangan (1998), whilst all of these methods also gave good estimates of the experimental findings with small standard deviations.

Nomenclature

C	compressive load on the concrete (N)
x	distance from extreme compression fibre to neutral axis (mm)
d	effective depth (mm)
d′	cover concrete (mm)
f_y	effective yield strength of rebars (MPa)
f_{su}	ultimate stress in reinforcing bar
l_s	splice length (mm)
M_1	theoretical ultimate moment due to compressive load (Nmm)
M_2	theoretical ultimate moment due to the tensile reinforcement (Nmm)
P	applied load (N)
T′	tensile load on the top reinforcement (N)

T_1 tensile load on the reinforcement due to compressive load (N)

T_2 tensile load on the reinforcement due to the compressive reinforcement (N)

u   average ultimate bond strength

z   distance between the resultant tensile and compressive loads (mm)

References

Azizinamini, A., Stark, M., Roller, J.J. and Ghosh, S.K., "Bond Performance of Reinforcing Bars Embedded in High-Strength Concrete", ACI Structural Journal, 90, 554-561, 1993.

Chan Y.W., Chen, Y.S. and Liu, Y.S., "Development of Bond Strength of Reinforcing Steel in Self-Consolidation Concrete", ACI Structural Journal, 100, 490-498, 2003.

Darwin, D., Zuo, J., Tholen, M.L. and Idun, E.K., "Development Length Criteria for Conventional and High Relative Rib Area Reinforcing Bars", ACI Structural Journal, 93, 347-359, 1996.

Dogangun, A., "Betonarme yapıların hesap ve tasarımı", Birsen Yayınevi, Turkey, 2003.

EFNARC, "European Guidelines for Self-Compacting Concrete", Specification and Production and Use, Association House,UK,(www.efnarc.org), 2005.

Esfahani, M.R., Lachemi, M. and Kianoush, M.R., "Top-Bar Effect of Steel Bars in Self-Consolidating Concrete (SCC)", Cement and Concrete Composite, 30, 52-60, 2008.

Esfahani, M.R. and Rangan, B.V., "Bond between Normal Strength and High-Strength Concrete and Reinforcing Bars in Splices in Beams", ACI Structural Journal, 95, 272-280, 1998.

Ezeldin, A.S. and Balaguru, P N. "Bond Behavior of Normal and High Strength Fiber-Reinforced Concrete", ACI Structural Journal, 86, 515-524, 1989.

Hoshino M., "Relationships between Bleeding, Coarse Aggregate, and Specimen Height of Concrete", ACI Materials Journal, 86, 185-190, 1989.

Hwang, S.J., Leu, Y.R. and Hwang, H.L., Tensile Bond Strengths of Deformed Bars of High-Performance Strength Concrete. ACI Structural Journal, 93, 11-20, 1996.

Okamura, H. and Ozawa, K., "Mix Design for Self-Compacting Concrete", Concrete Libr. JSCE, 25, 107-120, 1995.

Orangun, C.O., Jirsa, J.O. and Breen, J.E., "A Reevaluation of Test Data on Development Length and Splices", ACI Journal, 74, 114-122, 1977.

Turk, K., Caliskan, S. and Yildirim, M.S., "Influence of Loading Condition and Reinforcement Size on The Concrete / Reinforcement Bond Strength", Structural Engineering and Mechanics, 19, 337-346, 2005.

Turk, K. and Yildirim, M.S., "Bond Strength of Reinforcement in Splices in Beams", Structural Engineering and Mechanics, 16, 469-478, 2003.

Valcuende, M. and Para, C., "Bond Behaviour of Reinforcement in Self-Compacting Concretes", Construction and Building Materials, 23, 162-170, 2009.

Yerlici, V.A. and Özturan T., "Factor Affecting Anchorage Bond Strength in High-Performance Concrete", ACI Structural Journal, 97, 499-507, 2000.

Zhu, W., Sonebi, M. and Bartos, P.J.M., "Bond and Interfacial Properties of Reinforcement in Self-Compacting Concrete", Materials and Structures, 37, 442-448, 2004.